CHAPTER 5

ENHANCING THE PHOTOCATALYTIC ACTIVITY OF TiO_2 CO–DOPING OF GRAPHENE–Fe^{3+} IONS FOR FORMALDEHYDE REMOVAL

5.1 Introduction

In previous chapter, GR–TiO_2 (PTA) photocatalyst was successfully synthesized and the photocatalytic activity of GR–TiO_2 (PTA) with different weight ratios of graphene was examined. GR–TiO_2 (PTA, 1:50) performed larger photocatalytic activity in comparison with that of GR–TiO_2 (PTA, 1:10, 1:20 and 1:100). Graphene can be used as an adsorbent material to enhanced photocatalytic activity of TiO_2. The reduced band gap energy and the extendable absorption edge of light of the GR–TiO_2 photocatalyst are due to the formation of Ti–O–C bonds. The enhanced photocatalytic activity of GR–TiO_2 caused by preventing charge recombination can be clearly observed via the photocurrent density. Under UV or visible light irradiation, the photocurrent generation of GR–TiO_2 shows that GR–TiO_2 performs higher current density than that of TiO_2 because of its high conductivity from the π–π conjugation structure of carbon atoms.

Another way to improve the photocatalytic activity of TiO_2 in order to overcome limitations in the application of TiO_2 due to its properties is to extend the band gap energy of TiO_2 to a longer wavelength by doping with transition metal ions such as Fe^{3+}, Mn^{2+}, Ni^{2+}, Zn^{2+} and V^{5+} (Devi et al., 2010 and Wang et al., 2009). The Fe^{3+} dopant is considered to be a good transition metal to improve the photocatalytic activity of TiO_2 because the atomic radius of Fe^{3+} is close to that of Ti^{4+}. Therefore, Fe^{3+} can incorporate into the crystal structure of TiO_2 (Farhangi et al., 2011 and Lu et al., 2011). The stability of Fe^{3+} is another outstanding property resulting from its $3d^5$ electron configurations (Devi et al., 2010). The Fe^{3+}–doped TiO_2 photocatalyst exhibits greater photocatalytic activity in comparison with bare TiO_2; some authors have suggested that the increase in photocatalytic activity of Fe^{3+}–doped TiO_2 can be attributed to the prevention of electron/hole recombination (Elghniji et al., 2012). The photocatalytic activity of Fe^{3+}–TiO_2 is also enhanced by the redox reaction of Fe ions that can produce more $^{\bullet}OH$ and $^{\bullet}O_2^-$ radicals.

Formaldehyde (HCHO) is a volatile organic compound (VOCs) that causes irritation in human tissues such as the throat, and also causes headache and nausea (Sekine, 2002). It can be used as a target VOC to evaluate the photocatalytic activity of prepared GR/Fe^{3+}–TiO_2. HCHO is used as a raw material for urea–formaldehyde resin production and is commonly found in wood–based panels, textile fabrics, indoor furniture paints and combustion processes (Guimarães et al., 2012 and Rodrigues et al., 2012). Thus, the removal of HCHO is essential for improving air quality. Several indoor air cleaning methods have been developed to remove HCHO, such as biological treatment (Lu et al., 2012), adsorption (Pei and Zhang, 2011) and photooxidation (Boonamnunyvitaya and Photong, 2009). The photodegradation of HCHO in the presence of a TiO_2 photocatalyst is an outstanding technology because HCHO molecules are completely degraded to CO_2 and H_2O (Yang et al., 2007).

Owing to the small number of studies on the preparation and photocatalytic activity of the GR/Fe^{3+}–TiO_2 photocatalyst, the objective of this work was to prepare GR/Fe^{3+}–TiO_2 films and evaluate the effect of graphene and Fe^{3+} dopants on the photocatalytic activity of the TiO_2 photocatalyst. In this chapter, the effect of the Fe^{3+} dopant on the photocatalytic activity of GR/Fe^{3+}–TiO_2 for formaldehyde removal was evaluated by adding Fe^{3+} ions to GR–TiO_2 at different concentrations.

5.2 Results and discussion

5.2.1 Characterization

The results of crystalline structure including functional groups on the surface of TiO_2 and GR–TiO_2 (PTA) photocatalyst is the same similarity as that presented in Chapter 4. Briefly, TiO_2 nanoparticles that synthesized using PTA solution as a precursor have an anatase structure. The average crystal size calculated from Scherrer's equation is about 14.8 nm. The functional groups of the prepared TiO_2 (PTA), GR–TiO_2 (PTA) and graphene oxide were determined using FTIR as shown in Table 5.1.

Table 5.1 Functional groups of TiO_2 (PTA), GR–TiO_2 (PTA) and graphene oxide.

Sample	Functional group	Wavenumber (cm^{-1})
TiO_2 (PTA)	OH N–H Ti–O–Ti	3000–3600, 1632 1400 400–690
GR–TiO_2 (PTA)	OH N–H Ti–O–Ti and Ti–O–C	3000–3600, 1632 1400 790
Graphene oxide	OH C=O Epoxide (cyclic ether)	3420 and 1579 1723 1228

After UV-assisted photocatalytic reduction of the GR–TiO_2 (PTA) photocatalyst, the absorption peaks of the carbonyl and epoxide groups were not observed in the FTIR results of the GR–TiO_2 (PTA) photocatalyst. This implies that the carbonyl and epoxide groups in graphene oxide were completely reduced to graphene. The GR–TiO_2 photocatalyst at different weight ratios of graphene (1:100, 1:50, 1:20 and 1:10) were prepared and the photocatalytic activities of those catalysts were examined using methylene blue (MB) as an indicator (see Chapter 4). The results show that GR–TiO_2 (1:50) exhibited the highest photocatalytic activity than that of GR–TiO_2 (1:100, 1:20 and 1:10) including pure TiO_2. Therefore, the optimal amount of graphene added to TiO_2 is at the weight of 1:50.

5.2.2 Preliminary study of Fe^{3+} content in GR/Fe^{3+}–TiO_2 photocatalyst.

Iron (III) nitrate nonahydrate ($Fe(NO_3)_3 \cdot 9H_2O$) was added to the GR–TiO_2 sol with from 0 to 0.36 wt% Fe^{3+}. According to Table 5.2, Fe^{3+} ion that was added to GR–TiO_2 sol should be limited in the range of 0.06 to 0.18 wt% Fe^{3+}. The excessive Fe^{3+} ion in the range of 0.24–0.36 wt% leads turbid sol. Moreover, GR–TiO_2 sol was rapidly turned to turbid sol when the content of Fe^{3+} dopant is higher than 0.36 wt% and The GR–TiO_2 sol is suddenly precipitated by adding Fe^{3+} ion up to 0.60 wt%. Therefore, the amount of Fe^{3+} dopant added to GR–TiO_2 photocatalyst should be limited between 0.06–0.18 wt% Fe^{3+}.

Table 5.2 Stability of GR–TiO_2 sol at different weight ratio of Fe^{3+} ion.

Fe^{3+} (wt%)	GR–TiO_2
0.00	Transparent sol
0.06	Transparent sol
0.12	Transparent sol
0.18	Transparent sol
0.24	Turbid sol after 1 h
0.30	Turbid sol after 3 h
0.36	Turbid sol after 3 h
0.42–0.54	Turbid sol
0.60	Precipitate

5.2.3 The effect of the Fe^{3+} dopant on the GR–TiO_2 photocatalyst films

The equilibrium adsorption capacities of GR/Fe^{3+}–TiO_2 in comparison with those of TiO_2 and GR–TiO_2 photocatalyst films were 9.1, 11.0, 10.2, 10.6, 9.6 and 8.3 $mg_{(HCHO)}$ $g^{-1}_{(catalyst)}$, corresponding to TiO_2 (PTA), GR–TiO_2 (PTA, 1:50), GR/Fe^{3+}–TiO_2 (0.06 wt% Fe^{3+}), GR/Fe^{3+}–TiO_2 (0.12 wt% Fe^{3+}), GR/Fe^{3+}–TiO_2 (0.18 wt% Fe^{3+}) and Fe^{3+}–TiO_2 (0.12 wt% Fe^{3+}), respectively. The equilibrium adsorption capacity of the GR–TiO_2 and GR/Fe^{3+}–TiO_2 catalysts were greater than that of pure TiO_2 because of the added graphene. However, it was noted that the GR/Fe^{3+}–TiO_2 photocatalyst showed a slight decrease in equilibrium adsorption capacity when the weight fraction of the Fe^{3+} dopant increased. The photocatalytic activity of the GR/Fe^{3+}–TiO_2 photocatalyst films was evaluated using the decomposition of gaseous formaldehyde under UV and visible light irradiation. The effect of the percentage of the Fe^{3+} dopant on the photocatalytic activity of GR/Fe^{3+}–TiO_2 was examined, as shown in Figures 5.1 and 5.2.

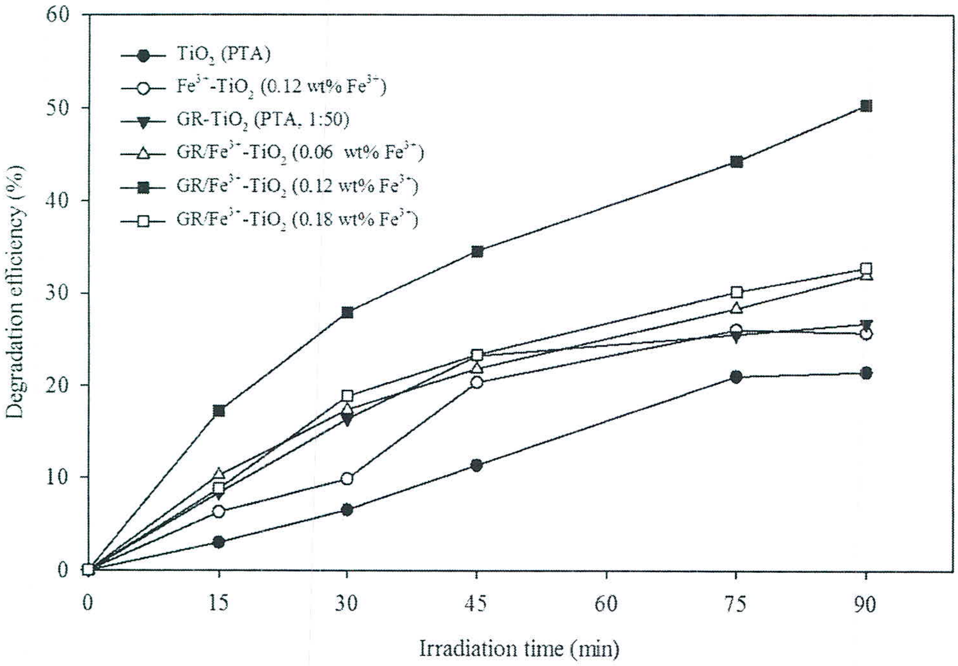

Figure 5.1 Degradation efficiency (%) of TiO_2, Fe^{3+}–TiO_2, GR–TiO_2 and GR/Fe^{3+}–TiO_2 at different weight ratios of Fe^{3+} ion under UV irradiation.

It was found that a small amount of the Fe^{3+} doping increased the photocatalytic activity of GR/Fe^{3+}–TiO_2 films with an increased percentage of the Fe^{3+} dopant until the maximum Fe^{3+} dopant concentration of 0.12 wt% was reached. However, an excess of the Fe^{3+} dopant in GR/Fe^{3+}–TiO_2 (0.18 wt%) led to a decrease in photocatalytic activity. Moreover, all GR/Fe^{3+}–TiO_2 catalysts performed with improved photocatalytic activity compared to pure TiO_2 and GR–TiO_2.

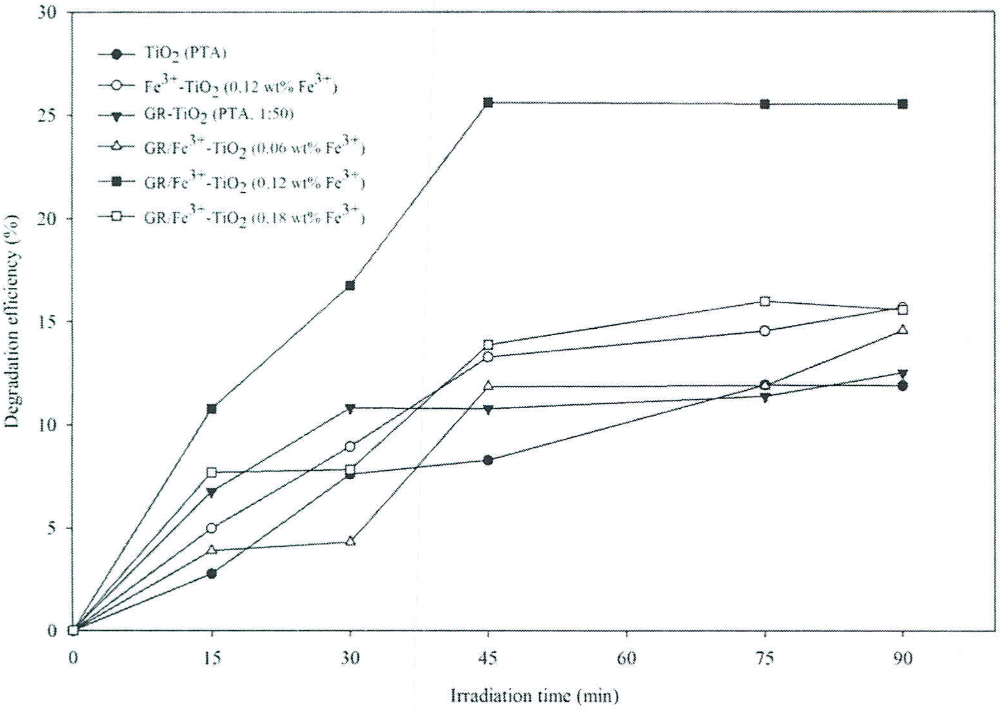

Figure 5.2 Degradation efficiency (%) of TiO_2, Fe^{3+}–TiO_2, GR–TiO_2 and GR/Fe^{3+}–TiO_2 at different weight ratios of Fe^{3+} ion under visible light irradiation.

The increase in photocatalytic activity of GR–TiO_2 was attributed to the large surface area of graphene. In the case of GR/Fe^{3+}–TiO_2, a trend for increased photocatalytic activity could be observed by increasing the weight ratio of Fe^{3+} ions. GR/Fe^{3+}–TiO_2 (0.12 wt% Fe^{3+}) exhibited the highest photocatalytic activity (UV and visible light) compared to the other catalysts. The decrease in HCHO degradation efficiency of GR/Fe^{3+}–TiO_2 (0.18 wt% Fe^{3+}) was lower than that of GR/Fe^{3+}–TiO_2 (0.12 wt% Fe^{3+}) and was ascribed to the recombination mechanism of Fe^{2+}/Fe^{3+} (Elghniji et al., 2012). It should be noted that the optimal weight ratio of the Fe^{3+} dopant in GR–TiO_2 was 0.12 wt%. The photocatalytic activity of Fe^{3+}–TiO_2 (0.12 wt% of Fe^{3+}) was not as high as that of GR/Fe^{3+}–TiO_2 (0.12 wt% Fe^{3+}). The greater photocatalytic activity of GR/Fe^{3+}–TiO_2 photocatalyst was attributed to the graphene and Fe^{3+} dopants. Generally, the spectra of GR–TiO_2 show a red shift in band gap transition more than that of pure TiO_2 because of the reduce band gap by the formation of Ti–O–C bond.

In the case of GR/Fe^{3+}–TiO_2 photocatalyst, the absorption edge shifted to visible light region more than that of GR–TiO_2 and TiO_2 photocatalysts. The absorption edge of catalysts from visible light to UV region can be ranged as follows: GR/Fe^{3+}–TiO_2 (0.18 wt% Fe^{3+}, 418 nm) > GR/Fe^{3+}–TiO_2 (0.12 wt% Fe^{3+}, 417 nm) > GR/Fe^{3+}–TiO_2 (0.06 wt% Fe^{3+}, 405 nm), GR–TiO_2 (394 nm) ≈ Fe^{3+}–TiO_2 (0.12 wt% Fe^{3+}, 394–390nm) > TiO_2 (388 nm). Figure 5.3 shows the shift in the absorption edge of the GR/Fe^{3+}–TiO_2 photocatalysts. A decrease in the band gap energy of the GR/Fe^{3+}–TiO_2 (0.12 wt% Fe^{3+}) photocatalysts was observed compared to that of GR–TiO_2 (PTA, 1:50) and Fe^{3+}–TiO_2 (0.12 wt% Fe^{3+}).

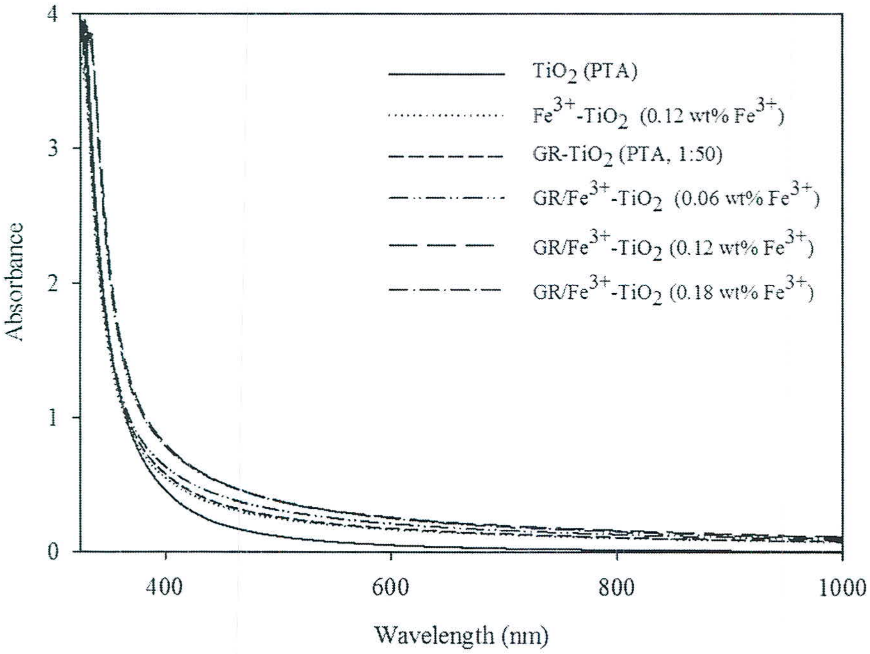

Figure 5.3 UV-vis absorption spectra of TiO_2 (PTA) and GR–TiO_2 (PTA) photocatalysts with different weight ratios of Fe^{3+} ion.

The decreasing in band gap energy of GR/Fe^{3+}–TiO_2 photocatalyst may attribute to the synergetic effect of the formation of the Fe^{2+}/Fe^{3+} energy line that forms below the conduction band of TiO_2 and the formation of the Ti–O–C bond as shown in Table 5.3.

Table 5.3 Estimated band gap energy of photocatalysts.

Sample	Estimated band gap (eV)
TiO_2 (PTA)	3.24
GR–TiO_2 (1:50)	3.20
GR/Fe^{3+}–TiO_2 (0.06 wt% Fe^{3+})	3.06
GR/Fe^{3+}–TiO_2 (0.12 wt% Fe^{3+})	2.97
GR/Fe^{3+}–TiO_2 (0.18 wt% Fe^{3+})	2.96
Fe^{3+}–TiO_2 (0.12 wt% Fe^{3+})	3.17

In order to understand the photocatalytic activity of GR/Fe^{3+}–TiO_2, the enhancement of photooxidation by adding the graphene and Fe^{3+} dopants should be separated into two parts: the effect of graphene and the effect of the Fe^{3+} dopant.

The effect of graphene on GR/Fe^{3+}–TiO_2 photocatalyst

Graphene can enhance the photocatalytic activity of GR/Fe^{3+}–TiO_2 by increasing the equilibrium adsorption capacity, preventing charge recombination and decreasing the band gap energy. The excited electrons from the valence band of TiO_2 can easily move to graphene because graphene has high conductivity property due to its π–π conjugation structure. This phenomenon can be clearly observed in photocurrent generation, as shown in Table 5.4. It was noted that the current densities of GR–TiO_2 and GR/Fe^{3+}–TiO_2 were higher than that of TiO_2.

The effect of Fe^{3+} dopant on GR/Fe^{3+}–TiO_2 photocatalyst

The effect of the Fe^{3+}dopant on the GR/Fe^{3+}–TiO_2 photocatalyst for gaseous formaldehyde removal was examined with a fixed graphene content in GR/Fe^{3+}–TiO_2 using an appropriate ratio between graphene and TiO_2 (1:50). GR/Fe^{3+}–TiO_2 (0.12 wt% Fe^{3+}) showed the best photocatalytic activity compared to TiO_2, GR–TiO_2 and GR/Fe^{3+}–TiO_2 (0.06 and 0.18wt% Fe^{3+}). The electron from the valence band was excited and moved to the conduction band of TiO_2 by photon absorption (Equation (5.1)). In the case of GR/Fe^{3+}–TiO_2, the additional mechanism of the Fe^{3+} dopant occurs, as Fe^{3+} ions can trap the excited electron from the valance band of TiO2, yielding Fe^{2+} (Equation (5.2)).

Table 5.4 Photocurrent generation of catalysts.

Sample	Current density ($\mu A\ cm^{-2}$)	
	UV irradiation	Visible light irradiation
TiO_2 (PTA)	2.90	2.30
GR–TiO_2 (1:50)	4.33	2.98
GR/Fe^{3+}–TiO_2 (0.06 wt% Fe^{3+})	9.80	6.27
GR/Fe^{3+}–TiO_2 (0.12 wt% Fe^{3+})	12.50	8.21
GR/Fe^{3+}–TiO_2 (0.18 wt% Fe^{3+})	5.32	3.80
Fe^{3+}–TiO_2 (0.12 wt% Fe^{3+})	5.12	3.37

However, Fe^{2+} is quite unstable compared to Fe^{3+} because Fe^{3+} has a half–filled d orbital (d^5) and the Fe^{2+} ion is relatively unstable because of its $3d^6$ electron configuration. Therefore, the Fe^{2+} ion will convert back to Fe^{3+} by transferring an electron to O_2 adsorbed on the surface of TiO_2 (Equation (5.4)). This process is called interfacial electron transfer. In addition, Fe^{3+} can act as a hole trap, resulting in Fe^{4+} that can produce hydroxyl radicals, as shown in Equation (5.3) and (5.5). The redox system of Fe^{3+}/Fe^{4+} can prevent the recombination of electron–hole pairs and leads to high photocurrent generation. However, a decrease in photocatalytic activity and photocurrent generation with GR/Fe^{3+}–TiO_2 (0.18 wt% Fe^{3+}) was observed because Fe^{3+} can also act as a recombination center for photo generated electrons and holes (Elghniji et al., 2012; Pang and Abdullah, 2012; Tieng et al., 2011 and Wang et al., 2011a).

$$TiO_2 + h\nu \longrightarrow e^- + h^+ \qquad (5.1)$$

$$Fe^{3+} + e^- \longrightarrow Fe^{2+} \qquad (5.2)$$

$$Fe^{3+} + h^+ \longrightarrow Fe^{4+} \qquad (5.3)$$

$$Fe^{2+} + O_{2ads} \longrightarrow Fe^{3+} + O_2^-{}_{ads} \qquad (5.4)$$

$$Fe^{4+} + OH^-_{ads} \longrightarrow Fe^{3+} + OH_{ads} \qquad (5.5)$$

$$Fe^{4+} + e^- \longrightarrow Fe^{3+} \qquad (5.6)$$

$$Fe^{2+} + h^+ \longrightarrow Fe^{3+} \qquad (5.7)$$

The absorption edge of the GR/Fe^{3+}–TiO_2 photocatalyst was extended to longer wavelengths and exhibited a lower band gap energy in comparison with that of GR–TiO_2 (1:50), which is an appropriate graphene content in TiO_2. This indicates that the band gap energy of GR/Fe^{3+}–TiO_2 was also reduced by adding Fe^{3+} ions. A Fe^{3+} ion in GR/Fe^{3+}–TiO_2 leads to an intra–band gap energy level close to the conduction band of TiO_2. Therefore, the double effects of graphene and Fe^{3+} ions can reduce the band gap energy by the formation of Ti–O–C bonds and the additional energy level below the conduction band of TiO_2 from Fe^{3+}/Fe^{2+} ions.

5.2.4 Repetitive use of the GR/Fe^{3+}–TiO_2 (0.12 wt% Fe^{3+}) photocatalyst

After the best conditions for the preparation of GR/Fe^{3+}–TiO_2 with the highest photocatalytic activity were achieved, the repeatability of the use of the GR/Fe^{3+}–TiO_2 (0.12 wt% Fe^{3+}) photocatalyst was investigated for real gaseous formaldehyde removal. Figure 5.4 shows the repeatability of the use of the GR/Fe^{3+}–TiO_2 (0.12 wt% Fe^{3+}) photocatalyst under UV and visible light irradiation. The results show that the average degradation efficiency after four cycles under UV was about 53.7 ± 2.6 % and 25.7 ± 1.2 % for visible light irradiation. The results indicate that the synthesized GR/Fe^{3+}–TiO_2 (0.12 wt% Fe^{3+}) photocatalyst film is suitable for air purification applications.

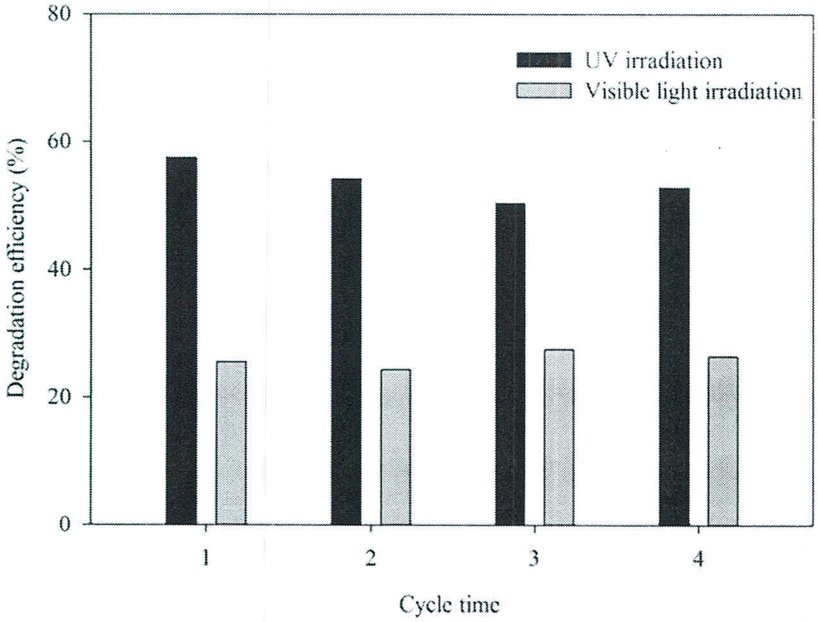

Figure 5.4 Repeatability of the use of GR/Fe^{3+}–TiO_2 (0.12 wt% Fe^{3+}) photocatalyst.

The adsorbed organic molecules on the surface of photocatalyst were degraded to CO_2 and H_2O. H_2O and O_2 can react with electron–hole pairs to produce $^{\bullet}OH$ and $^{\bullet}O_2^-$. Therefore, the adsorption sites on the surface of photocatalyst recovered itself by using photooxidation.

5.3 Conclusions

The GR–TiO_2 and GR/Fe^{3+}–TiO_2 photocatalysts were successfully synthesized. Graphene enhanced the photocatalytic activity of TiO_2 by increasing the adsorption property, suppressing charge recombination and reducing the band gap energy. In the case of GR/Fe^{3+}–TiO_2, it was noted that the Fe^{3+} dopant increases the photocatalytic activity compared to GR–TiO_2 with the same graphene content. The prevention of charge recombination increased the reaction of Fe^{3+} ions. Furthermore, the Fe^{3+} dopant led to an intra–band gap energy level which extended the absorption edge to the visible light region and reduced the band gap energy of GR/Fe^{3+}–TiO_2. The prepared GR/Fe^{3+}–TiO_2 (0.12 wt% Fe^{3+}) film can be applied as an effective photocatalyst to remove gaseous formaldehyde and it can be used several times.